Geomechanics and Engineering, *Vol. 22, No. 1 (2020) 1-9*
DOI: https://doi.org/10.12989/gae.2020.22.1.001

Ground response of a gob-side gateroad suffering mining-induced stress in an extra thick coal seam

Fulian He[1a], Sheng Gao[1,3b], Guangchao Zhang*[1,2,4] and Bangyou Jiang[2c]

[1]School of Energy and Mining Engineering, China University of Mining and Technology (Beijing), Beijing, 100083, China
[2]College of Energy and Mining Engineering, Shandong University of Science and Technology, Qingdao, 266590, China
[3]CCTEG Energy Technology Development Co., Ltd., Beijing, 100013, China
[4]Yankuang Group Co., Ltd., Zoucheng, 273500, China

(Received March 26, 2020, Revised May 9, 2020, Accepted May 18, 2020)

Abstract. This paper presents an investigation of the ground response of a gob-side gateroad suffering mining stress induced by a 21 m-thick coal seam extraction. A field observation, including entry convergence and stress changes monitoring, was first conducted in the tailgate 8209. The observation results of entry convergence showed that, during the adjacent panel 8210 retreating period, the deformation of the gob-side gateroad experienced a continuous increase stage, subsequently, an accelerating increase stage, and finally, a slow increase stage. However, strong ground response, including roof bending deflection, rib extrusion and floor heave, occurred during the current panel 8209 retreating period, and the maximum floor heave reached 1530 mm. The stress changes within coal mass of the two ribs demonstrated that the gateroad was always located in the stress concentrated area, which responsible for the strong response of the tailgate 8209. Subsequently, a hydraulic fracture technique was proposed to pre-fracture the two hard roofs above the tailgate 8209, thus decreasing the induced disturbance on the tailgate. The validity of the above roof treatment was verified via field application. The finding of this study could be a reference for understanding the stability control of the gob-side gateroad in extra thick coal seams mining.

Keywords: field observation; gob-side gateroads; mining-induced stress; hard and thick roofs; an extra thick coal seam

1. Introduction

Longwall top coal caving (LTCC) has been widely employed to extract thick coal seam (TCS) resources in China. However, a series of engineering problems have emerged when the LTCC mining is applied to full-height extraction of an extra thick coal seam (ETCS). Thereinto, ground control of gob-side gateroads has been one of the key technical problems in ETCS mining (Zhang *et al.* 2017). During ETCS mining, large-area overhangs strata emerged above the gob edge. Rotation and caving of such overhangs cause a stronger mining stress above the gob-side coal mass in a wider range (Basarir *et al.* 2015, Adhikary and Guo 2015). The above mining stress tends to stronger when the overlying strata includes hard massive stratum (Shabanimashcool and Li 2015). As a result, severe strata behaviors occurred in the gob-side gateroads, such as roof sag, floor heave, rib spalling etc. (Zhang *et al.* 2019, Zang *et al.* 2020). Given that, more attention should be paid to stability control of gob-side gateroads problems associated with disturbance induced by ETCS mining.

To date, considerable studies have been carried out to investigate the stability of gob-side gateroads in TCS mining, and various methods including experiment, analytical and modelling methods, have been developed. However, each approach suffers various limitations (Zhang *et al.* 2018, Wang *et al.* 2019, Oreste 2005). For example, the results obtained by experiments strongly depend on the testing procedure and equipment; the analytical methods are on the base of the hypotheses that the rock mass behaves elastically or plastically (Seo *et al.* 2016, Carranza-Torres 2009, Wang *et al.* 2020); In consideration of the complexity of the geological condition, it is difficult to obtain appropriate input parameters in a meticulously validated numerical model (Shnorhokian *et al.* 2014). We all known that ground performance of gateroads strongly depends on the site-specific geologic conditions and actual mining layout (Feng *et al.* 2019, Liu *et al.* 2020). Accurate evaluation of the gateroad performance can significantly contribute to gateroads stability improvements of future work (Li 2010). Therefore, field observation of gob-side gateroads performance is necessary and irreplaceable, even though it is costly and time-consuming. In recent years, considerable studies have been devoted to the stability analysis of gob-side gateroads by field observation methods in China. For instance, Bai *et al.* (2015), investigated the failure process of a gob-side entry suffering dynamic stress induced by the adjacent panel retreating. Zhang *et al.* (2020) carried a field observation of fracture development

*Corresponding author, Instructor
E-mail: 874557858@qq.com
[a]Professor
E-mail: fulianhe@sohu.com
[b]Ph.D.
E-mail: 928712841@qq.com
[c]Ph.D.
E-mail: jiangbangyou123@163.com

http://www.techno-press.org/?journal=gae&subpage=7 ISSN: 2005-307X (Print), 2092-6219 (Online)

in the coal/ rock mass surrounding the gob-side entry. Shen *et al.* (2018) and Bai *et al.* (2017) performed an comprehensive in situ investigation to assess the performance of coal pillars, respectively. Wang *et al.* (2018) conducted a field observation of the scope of excavation-damaged zones around the gateroad. In sum, field observation method can evaluate the gob-side gaterods performance objectively, and the obtained results are more trustworthy than those obtained by previous approaches. However, in fact, there are still some major weakness in their studies: (1) the previous studies are mainly on the coal seams with a thickness of less than 10 m, and there are very limited studies on gob-side gateroads in ETCS panels, especially for coal seam with a thickness nearly 20 m; (2) Traditionally, ground control of gob-side gateroads in TCS panels has been dealt with increasing supports strength or blasting the roof to relieve the high stress. However, in the ETCS mining, the enhanced supports cannot prevent the gateroads from the deformation and failure, and the blasting method poses a high risk of gas explosions and pressure (Qiu *et al.* 2019, Jiang *et al.* 2019). (3) of late, hydraulic fracturing technology is a promising and effective tool for the thick and hard roof treatment in TCS mining, but its application in ETCS remains in few. Given the weakness mentioned above, a comprehensive field observation is performed to assess the strong response of gob-side gateroads suffering mining-induced stress in ETCS panel, and validate the feasibility of roof treatment with hydraulic fracturing

In this paper, a coal mine located in Datong city, Shanxi Province, China, was selected for this case study. We implemented a comprehensive field observation to reveal the strong response of gob-side gateroads suffering mining disturbance induced by 21 m-thick coal seam extraction. We also attempted to deal with the thick hard roofs in ETCS panels with hydraulic fracturing; and its feasibility was verified by performing field applications. This study can help to get a better grasp of the ground stability of gob-side gateroads in ETCS mining.

2. Case study

2.1 Geological and mining condition

Madaotou (MDT) coal mine is located at the south of Datong city, Shanxi Province, China. Longwall panels 8209 and 8210 are used in this study. The panels are all 220 m along the strike and 1355 m along the dip. The geological column chart of panel 8209 is illustrated in Fig. 1. The mining coal seam is combined coal seam nos 3-5 with an average thickness and burial depth are 21.1m and 420m, respectively, and its average dip angle is 4°. The roof strata above the coal seam are, in ascending order, coarse sandstone (10.4 m) and medium-fine sandstone (11.6m), and the strata below the coal seam are, in descending order, mudstone (3.1 m) and medium-fine sandstone (6.5 m).

A fully mechanized top-coal caving mining longwall face was employed to extract the coal mass. The mechanized mining height and caving mining height were 3.9 m and 17.2 m, respectively. In actual engineering practice, for the purpose of achieving a coal mine production plan goal, the tailgate 8209 was completed prior to the extraction of panel 8210. Note that the coal pillar between tailgate 8209 and headgate 8210 is 30 m wide by 3.9 m high. Fig. 2 illustrates the layout of gateroass and panels. From the mechanical point of view, the tailgate 8209 will be loaded with the in situ stress during the gateroad development. Then, it will be loaded by the front abutment stress and the lateral abutment stress induced by panel 8210 retreating. During the panel 8210 retreating, the induced front abutment stress is also applied to the tailgate. Because of these dynamic and strong mining-induced disturbance, severe damage and deformation occurred in the field.

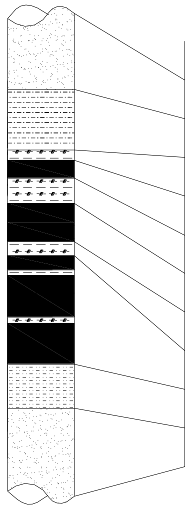

Thickness (m)	Depth (m)	Lithology
11.6	383.7	Medium-fine sandstone
10.4	395.3	Coarse sandstone
1.3	405.7	Mudstone
1.6	407.0	Coal seam #3
3.0	408.6	Mudstone
5.5	411.6	Coal seam #3-1
1.1	417.1	Mudstone
14.0	418.2	Coal seam #5
3.1	432.2	Mudstone
6.5	435.3	Medium-fine sandstone

Fig. 1 Generalized stratigraphy column of panel 8209

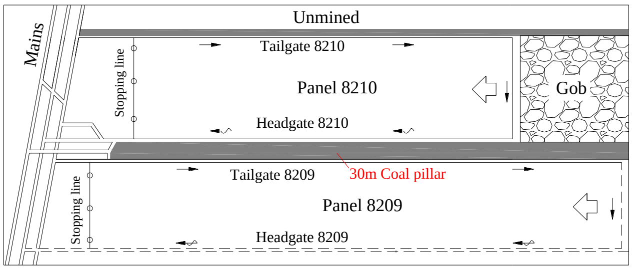

Fig. 2 Panel layout of the test site

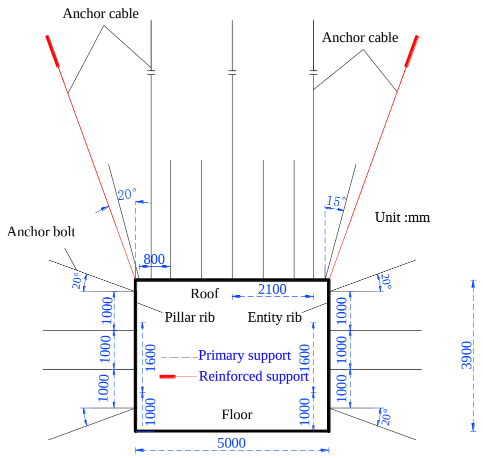

Fig. 3 Previous support scheme

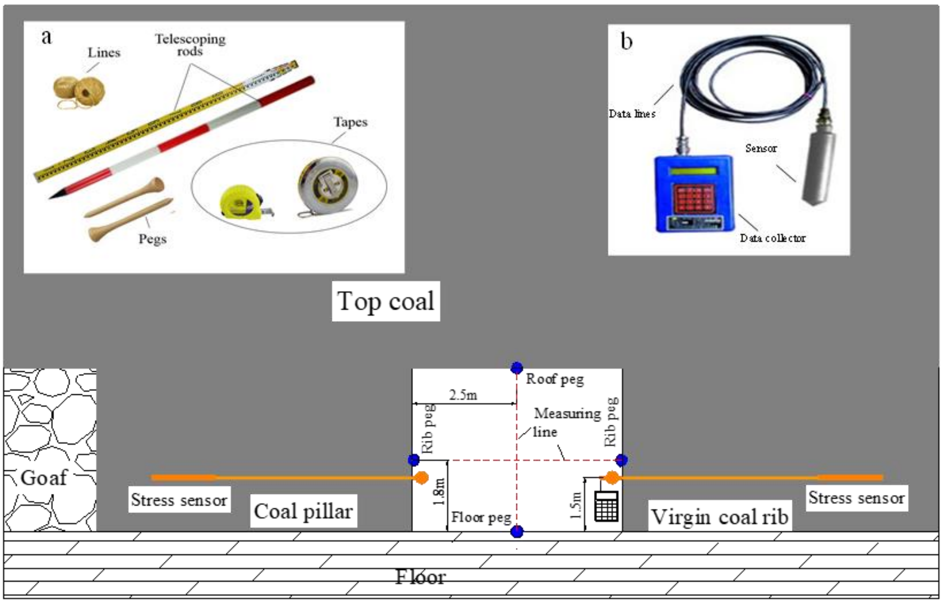

Fig. 4 Arrangement of the measurement station: (a) tapes, pegs, lines and telescoping rods and (b) extensometer system

2.2 Support scheme

The tailgate 8209 was 5.0 m wide and 3.9 m high, supported by bolts/cables, see Fig. 3. A 20 mm in diameter and 3100 mm long bolt was used in the roof support, and a 22 mm in diameter and 2400 mm long bolt was used in the two rib supports. The roof and ribs bolts were installed at a spacing of 800 mm × 900 mm and 1000 mm × 900 mm, respectively. The roof bolts were installed with steel mesh and a W-shaped steel strap for surface control. The rib support was installed with steel mesh and a steel channel for surface control. In addition, anchor cables were installed at the roof with a spacing of 2100 mm × 1800 mm. The cables were 21.8 mm in diameter and 8300 mm in length, and the cables were installed in a row on the same **I**-shaped steel beam.

During the panel 8210 retreat period, 21.8 mm in diameter and 4,500 mm long anchor cables (full line in red) were used in the roof reinforcement about 200 m ahead of the mining panel. The roof anchor cables were installed at a spacing of 5,000 mm × 1,800 mm.

3. Field observation

3.1 Field observation plan

During the tailgate 8209 development period, there existed no serious problems regarding roof falling, rib spalling, or floor heave. Therefore, we focused on the gateroad performance during panel 8210 and 8209 retreating period. A comprehensive field observation was performed in the tailgate 8209, as illustrated in Fig. 4. The details of the measurements, including the apparatus, its installation, and the data collection are described as follows:

• The roof-to-floor and rib-to-rib convergence were monitored by a flexible tape and telescoping rods, respectively. The roof and the floor pegs, installed in the mid-span of the roof and floor, were used to monitor roof-to-floor convergence, and the two rib pegs installed 1.8 m above the floor were used to detect rib-to-rib convergence. Noted that the instrumentation station was installed approximate 230 m in front of the setup room. The monitoring procedure lasted until the panel 8209 passed the station.

• The stress changes within the coal mass of the two ribs were detected by the ZKGYB stress. The six stress meters were installed in the coal pillar at depth of 3.5, 5.5, 10.5, 16.5, 22.5, and 28.5 m, respectively. And the other six meters were installed in the panel rib at depth of 5.5, 8.5, 11.5, 14.5, 17.5, and 20.5 m, respectively. All boreholes are drilled with a diameter of 56 mm and 1.5 m above the floor. All these meters were set up after panel 8210 was mined out, but before the panel 8209 retreated from its setup room.

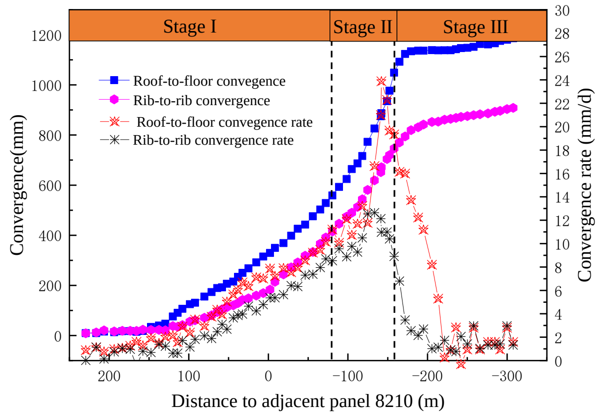

Fig. 5 Measured entry convergence of tailgate 8209 versus Panel 8210

3.2 Entry convergence analysis

Fig. 5 depicts the entry convergence and rate when the panel 8210 closed to the measurement station. The positive

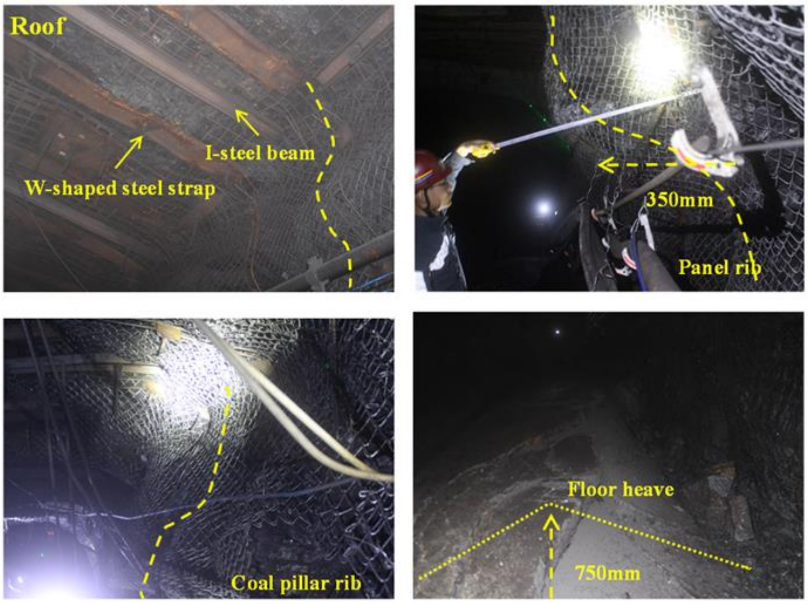

Fig. 6 Ground response of the tailgate 8209 during panel 8210 retreating

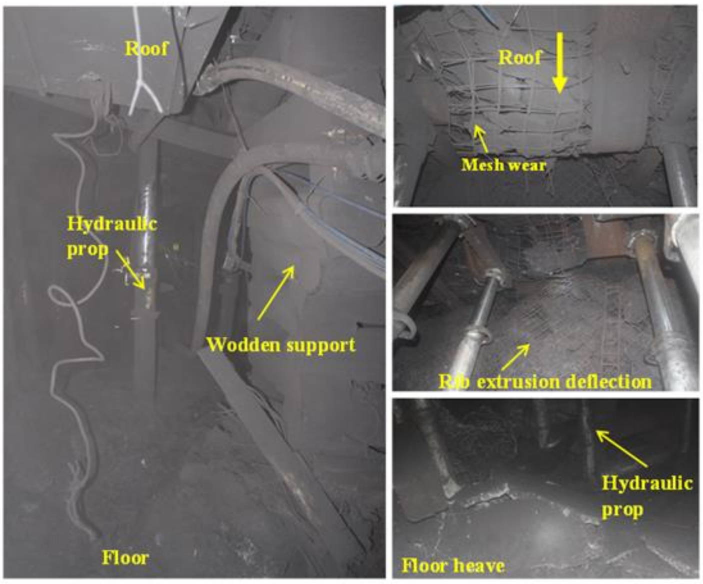

Fig. 7 Performance of the tailgate 8209 during panel 8209 retreating

numbers in the x-axis denote the station located in front of the panel 8210, while the negative numbers denote the station located behind of the panel 8210. In sum, based on the changes of entry convergence, the deformation and failure process of the gateroad can be divided into three stages: a continuous increase stage (Stage I), an accelerating increase stage (Stage II) and a slow increase stage (Stage III).

Stage I : The entry convergence magnitude and rate increased when the panel retreated closer from +220m in the front to -85 m behind of the station. When the panel retreated from +220 m to +120 m, the entry convergence increased gently with a daily convergence of 3-4 mm. About 0-120 m ahead of the mining panel, the convergence rate increased to 6-8 mm/day, continuing to increase up to 10-12 mm/day as the panel passed the station about 85 m. The cumulative roof-to-floor convergence reached 590 mm (height decrease 15.12%), and rib-to-rib convergence reached 446 mm (width reduction 8.92%).

Stage II : With advancing of the panel from -85 m to -160 m behind the panel, the entry convergence increases rapidly. The roof-to-floor and rib-to-rib convergence rate fluctuated at a range of 15-24 mm/day and 8-13 mm/day, respectively. The final deformation of roof-to-floor and rib-to-rib reaches 1093 mm (height decrease 28.02%) and 778 mm (width reduction 15.56%), respectively.

Stage III : With advancing of the panel from -160 m to -230 m behind the panel, the entry convergence increase gradually slowed down, and the roof-to-floor and rib-to-rib convergence rate decreased to 3-5 mm/d. The final deformation of roof-to-floor and rib-to-rib reaches 1184 mm (height decrease 30.35%) and 913 mm (width reduction 18.26%), respectively.

Fig. 6 presents the performance of tailgate 8209 during panel 8210 retreating. Field observations revealed the roof-coal mass performed relatively well, and deformations mostly occurred on the two ribs and floor strata. In some areas, the floor heave is significant with a maximum displacement of more than 750 mm, contributing more than 60% of the total roof-to-floor convergence. Overall, deformation and support component failures exist, but drastic failures were infrequently observed during panel 8210 retreat.

Fig. 6 presents the performance of tailgate 8209 during panel 8210 retreating. Field observations revealed the roof-coal mass performed relatively well, and deformations mostly occurred on the two ribs and floor strata. In some areas, the floor heave is significant with a maximum displacement of more than 750 mm, contributing more than 60% of the total roof-to-floor convergence. Overall, deformation and support component failures exist, but drastic failures were infrequently observed during panel 8210 retreat.

3.2.2 Gateroad performance during panel 8209 retreating

Fig. 7 presents the performance of the tailgate 8209 during panel 8209 retreating. It should be noted that, for the sake of safety, reinforced support, including hydraulic prop and woodden support, was applied in the field. Despite of this, severe roof sag, rib spalling and floor heave were observed frequently. Roof bending deflection occurred with a maximum displacement of 530 mm, resulting in the **I**-shaped steel beam or W-shaped steel strap bend. The coal mass of two ribs underwent a prominent extrusion deflection in the field, consequently resulting in the support system failure and rib spalling. The floor heave witnessed a sharply increase, and the maximum floor deformation reached 1530 mm. Due to the large deformation the roof and two ribs, the gateroad cross-section exhibited a tremendous reduction, resulting in a considerable amount of extra labour, financial resources and time loss.

3.3 Stress changes analysis

Fig. 8 illustrates the stress changes within the 30 m wide coal pillar during panel 8209 retreating. The x-axis refers to the relative distance between the panel 8209 and the meter-installed locations. For the stress meters at pillar depths of 3.5 m and 28.5 m, the stress reading kept a low value. For the stress at a pillar depth of 5.5m, the stress first increased gradually, and then decreased significantly; when the meter was 16m ahead of the mining panel, a maximum stress value of 7.65 MPa was reached. Similarly, the stress at a pillar depth of 25.5 m exhibited a similar changes tendency, and a maximum stress of 7.85 MPa was observed when it was 40 m ahead the mining panel. The above stress changes indicated that the coal mass at a coal pillar depth of 0-5.5 m and 25.5-30 m has been failed as the panel approached. For the stress changes at pillar depths of 10.5 m, 16.5 m and 22.5 m, the stress increase maintained a small rate when the panel retreating closer from 130 m to 60 m; then the

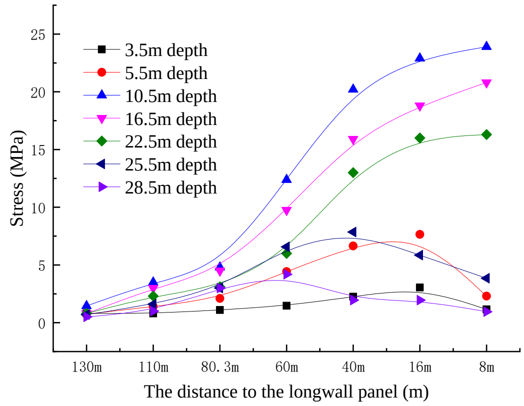

Fig. 8 Stress changes within the coal pillar during panel 8209 retreating

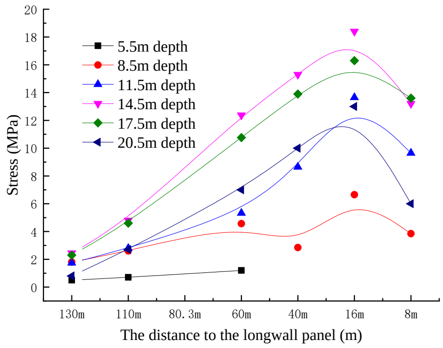

Fig. 9 Stress changes in panel rib at various depth versus the 8209 panel

increasing rate increased significantly when the panel retreated further from 60 m to 8 m. It can be concluded that there existed a high stress zone at pillar depth of 10.5-22.5 m, indicating that the inner coal body of coal pillar had an enough bearing capacity to undertake the roof vertical loads.

Fig. 9 illustrates the stress changes within the panel rib during panel 8209 retreating. Note that the reading of the stress meter at a depth of 5.5 m was unavailable when it was 8-60 m ahead mining panel, and it can be predicted that they could have been damaged before the measurement. The stress reading exhibited linearly increased as the panel retreated closer to the station from 130 m to 16 m. With the further retreat of the panel from 16 m to 5 m, the stress decreased significantly. The maximum stress reading was observed when the panel was 16 m ahead of the meter-installed location. Noted that compared to the stress value at other depths, the most of stress at a depth of 8.5m was generally low. This outcome indicated that coal mass on the panel rib side with a depth of 0-8.5 m has damaged to some degree.

4. Implications on ground stability of gob-side entries in ETCS

4.1 Failure mechanism analysis

The ground response of the entry is closely associated

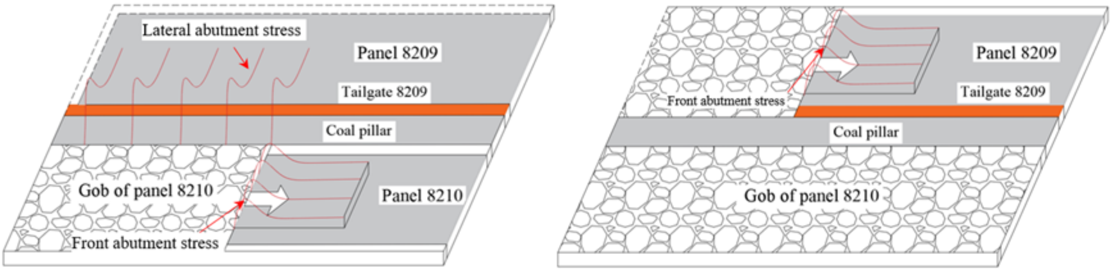

Fig. 10 Schematic plots of mining-induced stress at stage stage II and III

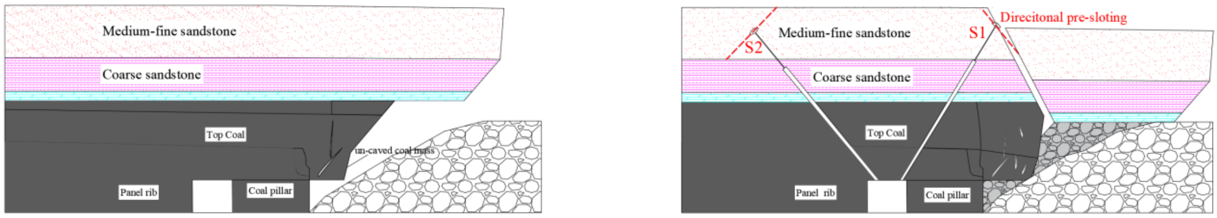

(a) Before hydraulic fracturing (b) After hydraulic fracturing

Fig. 11 Strata behaviors controlled with hydraulic fracture. (a) Before hydraulic fracturing and (b) After hydraulic fracturing

with the mining and excavation activities (Mohammadi *et al.* 2018). For the tailgate 8209, the underwent mining and excavation process can be divided into three stages: the development of the tailgate 8209, the retreating of the panel 8210 and the retreating of the panel 8209.

Stage I Development of the tailgate 8209. In this stage, the gateroad excavation resulted in stress redistribution, which causes the coal and rock masses deformed and failed gradually. Field observations indicated that the entry convergence in this stage is limited and can be controlled, which can be attributed to a high strength support (see Fig. 3) and a relatively small stress disturbance.

Stage II Retreat of the adjacent panel 8210. Due to the existing of hard massive stratum with a thickness of about 20 m (see Fig. 1), large-area overhangs strata emerged above the gob edge as the panel 8210 advanced. Thus, the stronger front abutment stress and the lateral abutment stress are created, see Fig. 10. According to the ground response of the tailgate 8209 and coal pillar width, it can be inferred that the tailgate 8209 is located at the lateral stress concentrated area. As a result, the entry convergence increases at a quickening pace in the field (see Fig. 4).

Stage III Retreat of the panel 8209. In this stage, the stress field balance was reactivated because of the retreat of panel 8210. Due to the large-area overhangs strata and the mining height nearly 21.1 m, the large impact loads induced by the fracture of the roof strata resulted in a large front abutment stress(Yavuz 2004), see Fig. 10. According to the numerical modelling results, the stress in the coal pillar and the panel rib reached 24.1 MPa and 18.3 MPa (Fig. 8 and 9), which was about 2.3 and 1.7 times the virgin stress, respectively. Affected by the higher stress, the gateroad suffered strong ground response (see Fig. 7).

In the mining and excavation process mentioned above, ground response of the tailgate 8209 was controlled mainly by the mining stress induced by panel 8209 retreating (*Stage III*); the mining-stress induced by panel 8210 retreating (Stage II) was then secondary, and the gateroad development induced stress (Stage I) was the least important.

4.2 Control strategy

The thick and hard hanging roofs are responsible for the high mining stress and the strong response of the gob-side gateroads at stage *II* and *III,* see Fig. 11(a). Currently, hard roof treatment using the hydraulic fracturing method is an effective method to decrease the mining-induced high stress (Huang *et al.* 2017). Additionally, the directional initiation of hydraulic cracks can be achieved by pre-slotting in the borehole in the field, as a result, hydraulic fractures reorient in three-dimension space.

The determination of the fracturing height of overhangs strata is a critical factor affecting the overall effectiveness of the hydraulic fracturing. Investigations have shown that if the caved coal and rock masses fill the gob area sufficiently, the stress concentration surrounding the gob-side gateroad can be relieved significantly because of considerable vertical loads will be carried out by the compacted caved coal and rock mass. Based on this, the minimum fracturing height can be estimated as follows:

$$h=\frac{M}{K_Z-1} \tag{1}$$

where M is the shearing mining height, and Kz is the average bulking factor of the caved coal and rock masses. For the specific geological condition of panel 8210, the mining height is 3.9 m, and the bulking factor is assumed to 1.30. Based on the above equation, the minimum fracturing height can be estimated as 13.0 m. According to the borehole column of panel 8209 and the delamination characteristics of the roof strata, the thickness of coarse sandstone and its below rock stratum is 11.7 m, less than 13.0 m. Therefore, the medium-fine sandstone was chosen to conduct hydraulic fracturing, to ensure the fracturing height s of the roof is more than 13.0 m

For the gob-side gateroad in this study, boreholes can be arranged as shown in Fig. 11(b). Boreholes S1 were drilled from the gob-side gateroad to the lateral over-hangs hard rock stratum above the gob area. The hydraulic fracturing is conducted at the medium-fine sandstone, and the pre-slotting is performed at the bottom of the boreholes along the inclination direction. After the application of directional hydraulic fracturing, with the support effectiveness of the un-caved coal mass in the intersection region, the fractured rock block fractured obliquely and slipped into the gob. Thus, the caved roof strata remove the stress-transferring media from the upper roofs, resulting in lower stress concentration in the adjacent coal pillar. Meanwhile, the caved roof strata produce sufficient waste to fill the mined-out space nearby the gob edge, which shares the overburden pressure and produces smaller failure zone in the coal pillar. In addition, boreholes S2 can be drilled before the current mining panel. As such, the hard roof can be cut off in advance so that it can cave in quickly behind the mining panel. Thereby, the front abutment stress can be eliminated significantly

5. Field test

5.1 Layout of the boreholes

Based on the gateroad performance of tailgate 8209 and the roof borehole columnar section, the detailed parameters of borehole are as follows, see Fig. 12. In order to reduce the mining-disturbance on tailgate 8209 to the most extent, all operations should be completed 200 m ahead of panel 8209. In the field, the hydraulic fracturing was carried out at a distance of 200~1000 m away from the stopping line.

Boreholes S1 are drilled at an elevation angle of 60°and toward the gob area of panel 8210 at 55°. The horizontal space between the adjacent boreholes is 20 m. According to the borehole columnar section of panel 8209, the 11.6 m thick Medium-fine sandstone was chosen to conduct hydraulic fracturing, so that the coarse sandstone (10.4 m in thickness) and medium-fine sandstone (11.6 m in thickness) can be cut off and caved sufficiently. Thereby, the depth of the borehole S1 can be estimated as 44 m. Boreholes S2 are drilled in the roof at an elevation angle of 85°and toward panel 8210 at 50°. The horizontal space between the adjacent boreholes is 20 m. The depth of the borehole S2 can be estimated as 46 m.

5.2 Construction procedure

The construction procedure in the field is described as follows:

(1) The boreholes are arranged as Fig. 12. The boreholes construction sequence is as follows. First, a borehole was drilled with a depth of 34~36 m and a diameter of 94 mm. Then, the borehole was drilled to a depth of 44~46 m with a diameter of 50 mm. Finally, the borehole wall was slotted directionally at the bottom. It should be noted that a contingent for borehole deformation should be reserved because of the severe damage of the 17.2-m-thick roof coal mass.

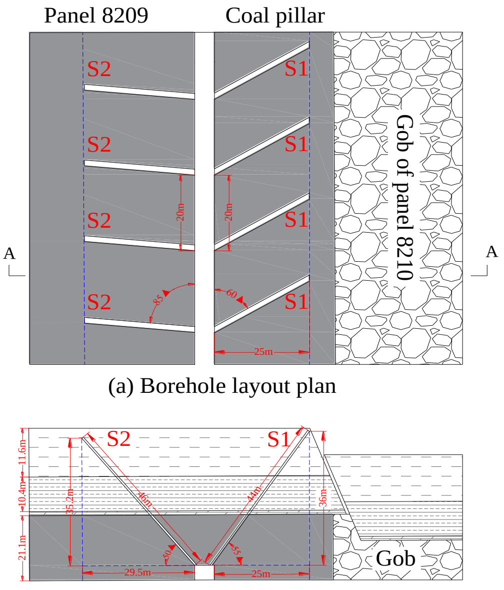

Fig. 12 Hydraulic fracture scheme used in tailgate 8209. (a) Borehole layout and (b)A-A profile

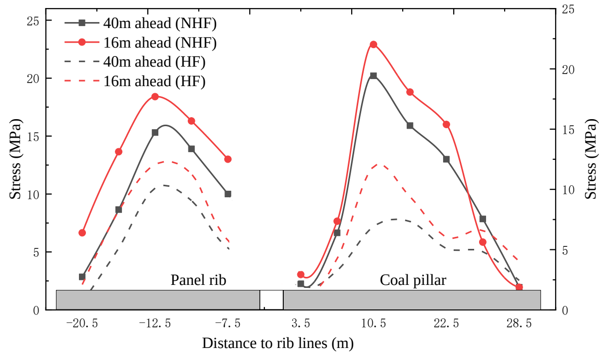

Fig. 13 Stress changes within two ribs in the scenarios of hydraulic fracturing (RS) and no hydraulic fracturing (NHF)

(2) The fracturing was performed by the hydraulic fracturing system, which includes BZW200 high-pressure pump, high-pressure pipes with a diameter of 19 mm, borehole packers with a diameter of 50 mm and mounting bar, etc. The packer together with mounting bar were fixed at the orifice, and connected with high-pressure pump by pipes. The water pressure was set as 50MPa during pumping. The working time of pumping was depending on the water pressure changes, the fracture time, etc.

(3) After the pumping was stopped, the packer together with mounting bar were dismounted from the boreholes, and reused for the next boreholes.

(4) Steps (1)-(3) were repeated until the all boreholes was implemented.

5.3 Monitoring results analysis

In order to assess the gateroad performance after

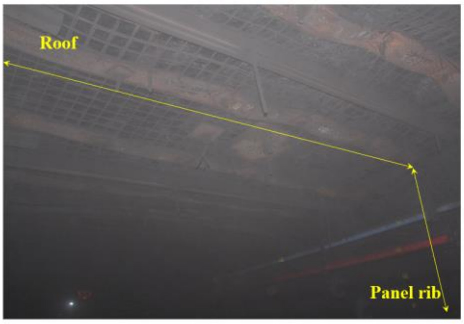

Fig. 14 Gateroad performance with hydraulic fracturing method

hydraulic fracturing, a field observation of stress changes and entry convergence was conducted in the test section. The detailed arrangement was similar to Fig. 4. Fig. 13 depicts the mining-induced stress in the gob-side gateroad after hydraulic fracturing scheme (HF). In comparing the conventional condition [e.g., no hydraulic fracturing (NHF)], the overall stress environment around the gob-side gateroad was improved to some degree. Although the stress distribution in the coal pillar and panel rib has similar tendency, but the peak stress in the coal pillar and panel rib decreased significantly.

Fig. 14 demonstrated that the gateroad performance significantly improved after hydraulic fracturing. The ground pressure was clearly lower than it was before hydraulic fracturing, and no significant rib spalling and floor heave were observed in the field. In total, the maximum convergence values of the entry roof, rib to rib and floor decreased to approximately 160, 230 and 340 mm by 69.81%, 60.85% and 77.2%, respectively. It can be inferred that hydraulic fracturing method can notably decrease the gob-side gateroad deformation.

6. Discussion

Currently, hard roof treatment using pre-splitting blasting or hydraulic fracturing method is the two most popular method to eliminate the mining-induced disturbance. Compared to the blasting method, the hydraulic fracturing poses the advantages such as smaller dynamic disturbance and good safety, especially in ETCS, for example 21 m thick coal seam in this study.

It should be noted that this study was only based on a specific coal mine model. In fact, the relevant parameters of hydraulic fracturing, such as borehole layout and water pressure design etc., are strongly depending on the geological and geotechnical conditions. And more case studies are necessary to deliver some general principles of hydraulic fracturing parameters design. However, the design principle and construction procedure presented in this study are necessary in the hydraulic fracturing implementation in other coal mines.

7. Conclusions

This study aimed to assess the ground response of a gob-side gateroad in ETCS panel extracting 21 m-thick coal seam based on a field observation, thus allowing the determination of a more effective ground control scheme with hydraulic fracturing. The main conclusions are as follows:

• Based on the results of the entry convergence and gateroad performance, mining disturbance of the adjacent panel retreating on the gateroad system started approximately 120 m ahead of the mining panel in the longitudinal direction and accelerated dramatically 85 m behind the mining panel. The mining-induced disturbance tend to stable about 230 m behind the panel.

• The stress monitoring results indicate that the high stress induced by panel retreating is responsible for the strong response of the tailgate 8209. The performance of tailgate 8209 is was dominated predominantly by panel 8209 retreating, and panel 8210 retreating was then secondary.

• Hydraulic fracturing method was employed to cut off the two hard hanging roofs above tailgate 8209, and the detailed parameters of borehole are determined. The improvement in gateroad stability could also be visually observed on site.

Acknowledgments

This study was supported by the National Natural Science Foundation of China (No.51974317 and 51904164), Yue Qi Distinguished Scholar Project (800015Z1138) China University of Mining & Technology (Beijing), Fundamental Research Funds for the Central Universities (800015J6), the Natural Science Foundation of Shandong Province (ZR2018QEE001).

References

Adhikary, D.P. and Guo, H. (2015), "Modelling of longwall Mining-Induced strata permeability change", *Rock Mech. Rock Eng.*, **48**(1), 345-359. https://doi.org/10.1007/s00603-014-0551-7.

Basarir, H., Ferid Oge, I. and Aydin, O. (2015), "Prediction of the stresses around main and tail gates during top coal caving by 3D numerical analysis", *Int. J. Rock Mech. Min. Sci.*, **76**, 88-97. https://doi.org/10.1016/j.ijrmms.2015.03.001.

Bai, J.B, Shen, W.L, Guo, G.W., Wang, X.Y. and Yu, Y. (2015), "Roof deformation, failure characteristics, and preventive techniques of Gob-Side entry driving heading adjacent to the advancing working face", *Rock Mech. Rock Eng.*, **48**(6), 2447-2458. https://doi.org/10.1007/s00603-015-0713-2.

Bai, Q.S., Tu, S.H., Wang, F.T. and Zhang, C. (2017), "Field and numerical investigations of gateroad system failure induced by hard roofs in a longwall top coal caving face", *Int. J. Coal Geol.*, **173**, 176-199. https://doi.org/10.1016/j.coal.2017.02.015.

Carranza-Torres, C. (2009), "Analytical and numerical study of the mechanics of rockbolt reinforcement around tunnels in rock masses", *Rock Mech. Rock Eng.*, **42**(2), 175-228. https://doi.org/10.1007/s00603-009-0178-2.

Feng, X.W., Zhang, N., Xue, F. and Xie, Z. (2019), "Practices, experience, and lessons learned based on field observations of support failures in some Chinese coal mines", *Int. J. Rock Mech. Min. Sci.*, **123**, 104097.

https://doi.org/10.1016/j.ijrmms.2019.104097.
Huang, B.X., Chen, S.L. and Zhao, X.L. (2017), "Hydraulic fracturing stress transfer methods to control the strong strata behaviours in gob-side gateroads of longwall mines", *Arab. J. Geosci*., **10**(11), 236. https://doi.org/10.1007/s12517-017-3024-y.
Jiang, B.Y., Gu, S.T., Wang, L.G., Zhang, G.C. and Li, W.L. (2019), "Strainburst process of marble in tunnel-excavation-induced stress path considering intermediate principal stress", *J. Central South Univ*., **26**(4), 984-999. https://doi.org/10.1007/s11771-019-4065-z.
Li, C.C. (2010), "Field observations of rock bolts in high stress rock masses", *Rock Mech. Rock Eng*., **43**(4), 491-496. https://doi.org/10.1007/s00603-009-0067-8.
Liu, Q., Chai, J., Chen, S.J., Zhang, D.D., Yuan, Q. and Wang, S. (2020), "Monitoring and correction of the stress in an anchor bolt based on pulse prepumped Brillouin optical time domain analysis", *Energy Sci. Eng*., 1-13. https://doi.org/10.1002/ese3.644.
Mohammadi, S., Ataei, M. and Kakaie, R. (2018), "Assessment of the importance of parameters affecting roof strata cavability in mechanized longwall mining", *Geotech. Geol. Eng*., **36**(4), 2667-2682. https://doi.org/10.1007/s10706-018-0490-2.
Oreste, P. (2005), "Back-analysis techniques for the improvement of the understanding of rock in underground constructions", *Tunn. Undergr. Sp. Technol*., **20**(1), 7-21. https://doi.org/10.1016/j.tust.2004.04.002.
Qiu, P.Q., Wang, J., Ning, J.G., Liu, X.S., Hu, S.C. and Gu, Q.H. (2019), "Rock burst criteria of deep residual coal pillars in an underground coal mine: A case study", *Geomech. Eng*., **19**(6), 499-511. https://doi.org/10.12989/gae.2019.19.6.499.
Seo, H., Choi, H. and Lee, I. (2016), "Numerical and experimental investigation of pillar reinforcement with pressurized grouting and pre-stress", *Tunn. Undergr. Sp. Technol*., **54**, 135-144. https://doi.org/10.1016/j.tust.2015.10.018.
Shabanimashcool, M. and Li, C.C. (2015), "Analytical approaches for studying the stability of laminated roof strata", *Int. J. Rock Mech. Min. Sci*., **79**, 99-108. https://doi.org/10.1016/j.ijrmms.2015.06.007.
Shen, W.L., Bai, J.B., Li, W.F. and Wang, X.Y. (2018), "Prediction of relative displacement for entry roof with weak plane under the effect of mining abutment stress", *Tunn. Undergr. Sp. Technol*., **71**, 309-317. https://doi.org/10.1016/j.tust.2017.08.023.
Shnorhokian, S., Mitri, H.S. and Thibodeau, D. (2014), "A methodology for calibrating numerical models with a heterogeneous rockmass", *Int. J. Rock Mech. Min. Sci*., **70**, 353-367. https://doi.org/10.1016/j.ijrmms.2014.05.011.
Wang, H.W., Xue, S., Jiang, Y.D., Deng, D., Shi, S. and Zhang, D. (2018), "Field investigation of a roof fall accident and large roadway deformation under geologically complex conditions in an underground coal mine", *Rock Mech. Rock Eng*., **51**(6), 1863-1883. https://doi.org/10.1007/s00603-018-1425-1.
Wang, J., Ning, J.G., Qiu, P.Q., Yang, S. and Shang, H.F. (2019), "Microseismic monitoring and its precursory parameter of hard roof collapse in longwall faces: A case study", *Geomech. Eng*., **17**(4), 375-383. https://doi.org/0.12989/gae.2019.17.4.375.
Wang, J., Qiu, P.Q., Ning, J.G., Zhuang L. and Yang, S. (2020), "A numerical study of the mining-induced energy redistribution in a coal seam adjacent to an extracted coal panel during longwall face mining: A case study", *Energy Sci. Eng*., **8**(3), 817-835. https://doi.org/10.1002/ese3.553.
Yavuz, H. (2004), "An estimation method for cover pressure re-establishment distance and pressure distribution in the goaf of longwall coal mines", *Int. J. Rock Mech. Min. Sci*., **41**(2), 193-205. https://doi.org/10.1016/S1365-1609(03)00082-0.
Zang, C.W., Chen, M., Zhang, G.C., Wang, K. and Gu, D.D. (2020), "Research on the failure process and stability control technology in a deep roadway: Numerical simulation and field test", *Energy Sci. Eng*. https://doi.org/10.1002/ese3.664.
Zhang, G.C., Chen, L.J., Wen, Z.J., Chen, M., Tao, G.Z., Li, Y. and Zuo, H. (2020), "Squeezing failure behavior of roof-coal masses in a gob-side entry driven under unstable overlying strata", *Energy Sci. Eng*. https://doi.org/10.1002/ese3.678.
Zhang, G.C., He F.L., Jia H.G. and Lai Y.H. (2017), "Analysis of gateroad stability in relation to yield pillar size: A case study", *Rock Mech. Rock Eng*., **50**(5), 1263-1278. https://doi.org/10.1007/s00603-016-1155-1.
Zhang, G.C., Tan, Y.L., Liang, S.J. and Jia, H.G. (2018), "Numerical estimation of suitable Gob-Side filling wall width in a highly gassy longwall mining panel", *Int. J. Geomech*., **18**(8), 04018091. https://doi.org/10.1061/(ASCE)GM.1943-5622.0001217.
Zhang, G.C., Wen, Z.J., Liang, S.J., Tan, Y.L., Tian, L., Zhao, Y. Q. and Zhao, D.S. (2019), "Ground response of a gob-side entry in a longwall panel extracting 17 m-Thick coal seam: A case study", *Rock Mech. Rock Eng*., **53**, 497-516. https://doi.org/10.1007/s00603-019-01922-5.

CC